Journal of Power Sources 196 (2011) 1521–1529

Contents lists available at ScienceDirect

Journal of Power Sources

journal homepage: www.elsevier.com/locate/jpowsour

Optimal arrangement for through-holes in a three-dimensional thin-film battery

A. Averbuch[a], M. Nathan[b,*], I. Sedelnikov[a]

[a] School of Computer Science, Tel Aviv University, Tel Aviv 69978, Israel
[b] School of Electrical Engineering, Tel Aviv University, Tel Aviv 69978, Israel

ARTICLE INFO

Article history:
Received 26 July 2010
Accepted 23 August 2010

Keywords:
3D
Thin-film
Batteries
Capacitors

ABSTRACT

In 3D thin-film batteries (3D-TFBs) and in trenched capacitors, the surface area is increased by forming holes in a substrate such as a silicon wafer. In this paper we define area gain (AG) as a ratio of the total new surface area (including the surface areas of all the holes) to the original surface area of the substrate ("footprint"). We analyze the AG for different configurations of convex polygonal holes within the substrate. In most cases, the AG can be computed based on the P/S ratio, where P is the sum of all hole perimeters and S is the surface area of one side of the substrate. Assuming that the diameter of each hole is not less than D and that the distance between any two holes is not less than s, the P/S ratio never exceeds $4/(D+2s)$. Tesselation of the surface into a regular grid of polygonal cells of diameter $D+s$ with regular polygonal holes of the same form (of diameter D) results in $P/S = 4D/(D+s)^2$. We propose two alternative tessellations (one with regular square holes and another with regular triangular holes) which have P/S ratios slightly better than $4D/(D+s)^2$ and which satisfy the assumptions of the hole diameter and the wall width. It is found that a smoothed triangular tessellation provides the largest AG.

1. Introduction

Three-dimensional (3D) thin-film batteries [1–3], also referred to as "3D TFBs", are a new class of batteries that combine the power advantages of planar (2D) TFBs with more that an order of magnitude increase in areal and volumetric energies and capacities vs. such planar TFBs. A 3D TFB is fabricated on a substrate perforated with an array of through-holes having a high aspect (length-to-diameter) ratio. Typically, the aspect ratio is 10:1. In a configuration in which a full battery is formed in each hole, thin films are deposited conformally on all available surfaces, see Fig. 1. The final structure is one of tens of thousands of concentric microbatteries per cm^2, connected in parallel. Rechargeable Li-ion 3D TFBs have been fabricated on glass (microchannel plates) and silicon substrates and testing has proved their vastly superior performance per cm^2 "footprint" relative to state-of-the art 2D TFBs [4–7]. A recent paper reviews the literature on both 2D and 3D TFBs and evaluates their potential use as power sources for implantable medical devices [8]. It is notable that in addition to the development of conformal deposition techniques which use essentially wet chemistry (electroless and electrodeposition), as done in Refs. [2–8], a group at Philips is pursuing the fabrication of 3D TFBs in non-through-holes using vacuum deposition (essentially CVD) techniques [9,10]. The following is described with reference to a silicon substrate (also referred to as wafer or chip).

Since the improvement in "performance per footprint" is strongly related to the aspect ratio and the geometrical arrangement of the through-holes, the aim of this study was to find the form and the arrangement of holes that maximizes the surface area, under the condition that this configuration can be implemented in practice. Practical constraints imposed by the fabrication process include:

- The hole diameter needs to be sufficiently large to allow free flow/insertion of liquids (or polymers used as separators) used in the deposition processes.
- The surface of the hole walls needs to be "sufficiently smooth" so that the layers are uniform in thickness.
- There is a lower bound on the possible width of the wall between two adjacent holes and between a hole and the substrate edge.

The notion of area gain (AG) is introduced to measure the efficiency of each configuration. The AG is defined as the ratio of the useful surface to the area S of one (top or bottom) side of the substrate. The substrate is assumed to be a flat plate and S is the area of one of its sides. The "useful surface" depends not only on the form of the substrate, but also on the form and configuration of the holes and on the location of the layers. For example, if a full substrate (without holes) is used and layers are deposited only on one of its sides, then AG = 1. If both sides are used, AG = 2. If layers are deposited also on the border of the wafer/chip, then the

* Corresponding author. Tel.: +972 3 6407027; fax: +972 3 6423508.
E-mail address: nathan@eng.tau.ac.il (M. Nathan).

0378-7753/$ – see front matter © 2010 Elsevier B.V. All rights reserved.
doi:10.1016/j.jpowsour.2010.08.059

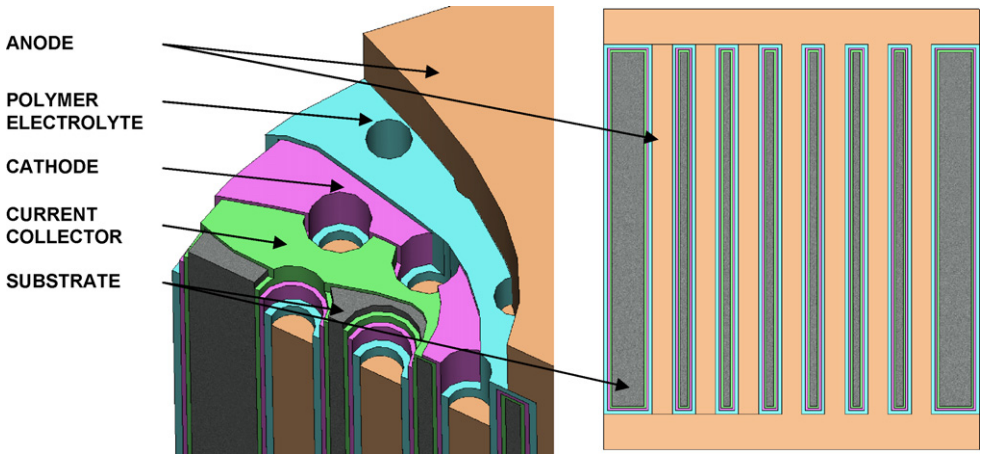

Fig. 1. Structure of 3D microbattery.

area gain equals $(2S + Ld)/S = 2 + Ld/S$, where L is the perimeter of the wafer/chip and d is the hole length (equal to the substrate thickness in the case of through-holes).

2. Formalization of the problem

When vertical holes are formed in a planar substrate, the additional "internal" hole surface area on which battery layers can be formed equals Pd, where P is the sum of perimeters of all the holes. The ratio between this internal area and the area S equals $(P/S)d$. If only the walls of the holes are covered with cathode/anode layers, then $AG = (P/S)d$. If the remaining planar surface of the substrate is also covered with cathode/anode layers, the AG increases. It is also possible to create non-penetrating holes (as in the silicon substrates in [9]), leaving a thin layer of silicon parallel to the surface, Fig. 2, in which case $AG = (2S + Pd)/S = 2 + (P/S)d$. In both cases, for a fixed d, the AG can be computed using the P/S ratio. Therefore, our goal is to find the configuration and the form of holes that maximizes the P/S ratio under the constraints listed above. Since it is difficult to formalize these requirements in a unique way, we will consider the following formalization: The holes are convex polygons with a specified minimal diameter D (diameter of a circle which can be placed inside the polygon). The diameter is chosen to allow the free flow of liquid. A "sufficiently uniform" distribution of the deposited material is ensured since the walls of the convex polygon are smooth. There is a minimal inter-hole wall width s, which means that the distance between any two points of any two polygons is at least s. We also require that the distance between any polygon and the substrate edge be at least $s/2$. In fact, the estimates on the P/S ratio obtained for convex polygons will hold for arbitrary convex holes that satisfy the same constraints, because any convex object can be approximated by convex polygons to an arbitrary degree of precision.

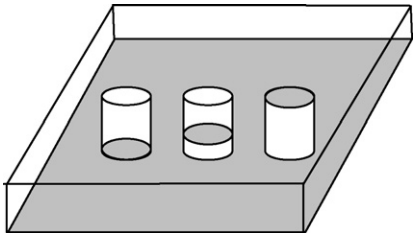

Fig. 2. Non-penetrating holes: a thin substrate section parallel to the surface is left inside each hole.

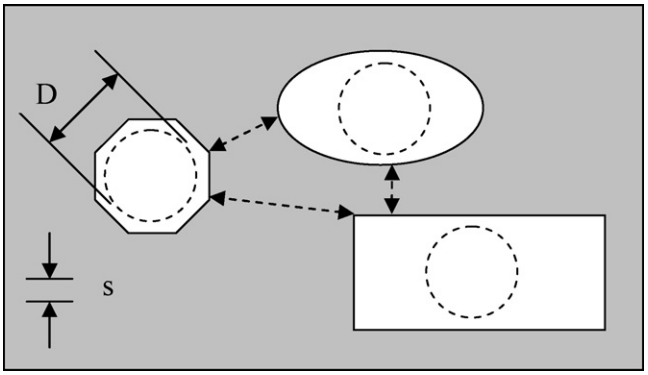

Fig. 3. Possible configurations of polygonal holes.

2.1. Convex polygonal holes

Fig. 3 illustrates a possible configuration of polygonal holes in the substrate. For any configuration that satisfies the requirement that the minimal wall width is not less than s, we can tessellate the silicon surface into a set of closed cells with walls of width not less than $s/2$, as shown in Fig. 4. S is the sum of areas of all the cells in the tessellation. Since the whole silicon area is covered by cells, the sum of areas of all cells equals the area of one side of the silicon plate, which is exactly the definition of S given earlier.

In order to maximize the P/S ratio, we first establish for it an upper bound under the assumption that walls can be arbitrarily thin, then check the case in which the width of the walls is at least

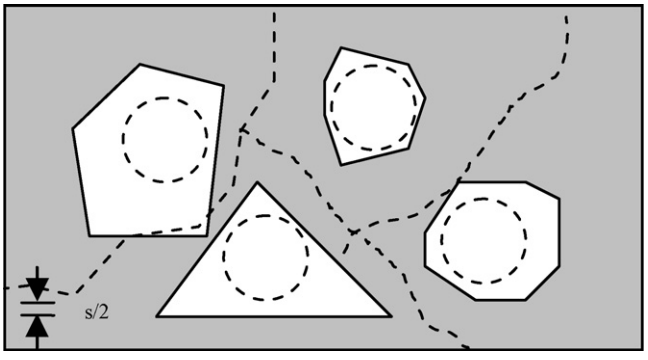

Fig. 4. Tessellation of a substrate surface into a set of closed cells with walls of width not less than $s/2$.

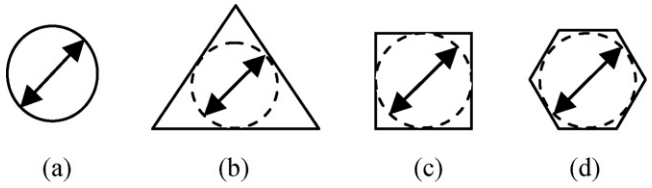

Fig. 5. (a) Circle of diameter D. (b) Triangle with inscribed circle of diameter D. (c) Square with inscribed circle of diameter D. (d) Hexagon with inscribed circle of diameter D.

s. Before we begin the analysis of the whole tessellation, it is helpful to study the P/S ratio for a single cell.

2.2. P/S ratio for a convex polygonal cell

Consider a convex polygon which contains a circle of diameter D (Fig. 5a). We first find the P/S ratio for this circle and for some simple polygons, see Fig. 5a–d. The polygons are: (a) a circle of diameter D: $P_0 = \pi D$, $S_0 = (\pi/4)D^2$, $P_0/S_0 = 4/D$; (b) a triangle with an inscribed circle of diameter D: $P_3 = 3\sqrt{3}D$, $S_3 = (3\sqrt{3}/4)D^2$, $P_3/S_3 = 4/D$; (c) a square with an inscribed circle of diameter D: $P_4 = 4D$, $S_4 = D^2$, $P_4/S_4 = 4/D$; and (d) a hexagon with an inscribed circle of diameter D: $P_6 = 2\sqrt{3}D$, $S_6 = (\sqrt{3}/2)D^2$, $(P_6/S_6) = 4/D$; In Appendix A, we prove the following results (Lemmas 3 and 4):

- For a regular polygon with inscribed circle of diameter D and perimeter P, $P/S = 4/D$.
- For a convex polygon containing a circle of diameter D, $P/S \le 4/D$.
- For a convex polygon containing a circle of diameter D, the equality $P/S = 4/D$ holds if and only if the polygon is formed by lines tangent to the circle.

2.3. P/S ratio for tiling with convex polygons

We now compute an upper bound for tessellation ("tiling") of a silicon wafer to cells, such that every cell contains a convex polygonal hole of at least internal diameter D. We start with the assumption that it is possible to create infinitely thin walls. In this case, P equals the sum of the perimeters of all the holes, and S is greater than or equal to the sum of the areas of all the holes. Then, by Lemma 5 in Appendix A we have $P/S \le 4/D$.

2.4. Non-zero width walls

Next, we consider tessellations where the distance between two neighboring holes is at least s, and where the distance from any hole to the substrate edge is at least $s/2$. As we already noted earlier, in this case, the substrate surface can be subdivided (tesselated) into cells, such that each cell contains one convex polygonal hole and the distance from any point of the hole to the border of the cell is at least $s/2$.

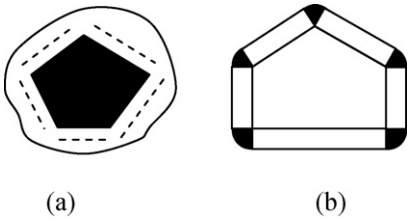

Fig. 6. (a) Polygonal hole. Dashed lines are located at the distance $s/2$ from the hole walls. (b) A strip of width $s/2$ around the polygonal hole.

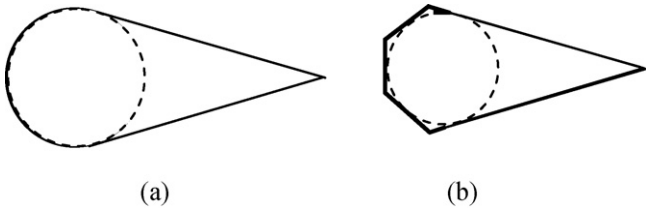

Fig. 7. (a) A polygon that has lines tangent to the circle. (b) A convex polygon that has sides tangent to the circle.

2.5. P/S for a cell

Next, we consider cells with a convex polygonal hole and walls of width not less than $s/2$, where a circle of diameter D can be placed inside the hole. Let P denote the perimeter of the hole, S_H the hole area, and S the cell area. Then, as seen in Fig. 6a, we have $S \ge S_H + P(s/2)$. By Lemma 4 in Appendix A, we have $P/S_H \le 4/D$. Applying Lemma 6, we get $P/S \le 4/(D+2s)$.

It is possible to provide a tighter estimate. For a given convex polygonal hole, the cell of the least area is the cell whose boundary consists of all points at distance less than or equal to $s/2$ from the hole. Since the area of the cell is minimal, the P/S ratio is maximal (for a given specific hole). Fig. 6b is a strip of width $s/2$ around a convex polygon. Consider an arbitrary vertex in this polygon. Denote the inner angle by α. Then, the angle, which is marked in black in Fig. 6b, is $360 - \alpha - 90 - 90 = 180 - \alpha$. The sum of all the inner angles of a convex N-sided polygon is $(N-2)\cdot 180^\circ$. Consequently, the sum of all the angles in Fig. 6b is $\sum_{i=1}^{N}(180 - \alpha_i) = N \cdot 180^\circ - \sum_{i=1}^{N}\alpha_i = 360^\circ$. Therefore, the area of all the black sectors in Fig. 6b is $\pi(s/2)^2$ and $S = S_H + P(s/2) + \pi(s/2)^2$. Consequently, the best P/S ratio for any cell with convex polygonal hole of perimeter P is $P/S = P/(S_H + P(s/2) + \pi(s/2)^2)$. By Lemma 4, we have $P/S_H \le 4/D$. Therefore, $S_H \ge PD/4$. When we substitute it into the P/S estimate, we get $P/S \le P/((PD/4) + P(s/2) + \pi(s/2)^2)$. Thus, $P/S \le 4P/(P(D+2s) + \pi s^2)$. An equivalent expression is $P/S \le (4/(D+2s))(1 - ((\pi s^2)/(P(D+2s) + \pi s^2)))$. In this form, we see that this estimate is tighter than $P/S \le 4/(D+2s)$, because the expression in the brackets is always less than 1.

In summary, for a cell which consists of a convex polygonal hole of perimeter P and walls of exact $s/2$ width, we have the following results:

- $\frac{P}{S} \le \frac{4}{D+2s}$
- $\frac{P}{S} = \frac{P}{S_H + P(s/2) + \pi(s/2)^2}$
- $\frac{P}{S} \le \frac{4P}{P(D+2s)+\pi s^2}$ or equivalently $\frac{P}{S} \le \frac{4}{(D+2s)}\left(1 - \frac{\pi s^2}{P(D+2s)+\pi s^2}\right)$.

We see that the right-hand side of the second result (equality) depends on the area S_H of the hole. The smaller S_H, the higher the P/S ratio.

How small can S_H be made for a fixed P? From Lemma 4, we know that $P/S_H \le 4/D$, that is $S_H \ge PD/4$. From the same lemma we know that $P/S_H = 4/D$ when the polygon is formed by lines tangent

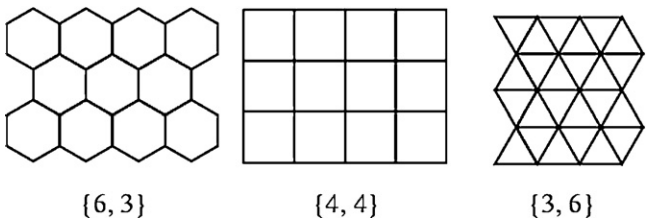

Fig. 8. Three possible regular tessellations of the plane: Left: hexagons. Middle: squares. Right: triangles.

to the circle. We claim that for any perimeter $P > \pi D$, we can find such a polygon. Although we give no formal proof, we provide an argument why this is true. Indeed, for an arbitrary $P > \pi D$, we can form Fig. 7a, which has a perimeter $P-\varepsilon$ for a small positive ε. Then, we can build a convex polygon with sides which are tangent to the circle of the form shown in Fig. 7b with perimeter P (this claim is left without formal proof). This means that for any $P > \pi D$, we can find a convex polygon which contains a circle of radius D such that $P/S = P/((PD/4) + P(s/2) + \pi(s/2)^2) = 4P/(P(D+2s) + \pi s^2)$, which shows that the estimate $P/S \le 4P/(P(D+2s) + \pi s^2)$ for a single cell is tight. We get $P/S = 4/((D+2s) + (\pi/P)s^2)$. It is easy to see that when $P \to \infty$ the P/S ratio converges to the familiar "coarse" estimate $4/(D+2s)$.

2.6. P/S for tessellation

Once we have an estimated P/S ratio for a single cell, we analyze the P/S ratio of the whole tessellation. As noted earlier, the substrate surface can be subdivided into cells such that each cell contains one convex polygonal hole with an inner diameter of at least D. The distance from any point in the hole to the border of the cell is at least $s/2$. Suppose that there are N cells in this subdivision. We enumerate them and denote by P_i the perimeter of the polygon contained in the ith cell, by S_i^H the area of the polygon, and by S_i the area of the ith cell. Above, we showed that $P_i/S_i \le 4/(D+2s)$ for any $i \in \{1, ..., N\}$. Then, by Lemma 2 in Appendix A we get the estimate $P/S \le 4/(D+2s)$, where $P = \sum_{i=1}^{N} P_i$ is the sum of the perimeters of all the holes and $S = \sum_{i=1}^{N} S_i$ is the sum of the areas of all the cells, i.e. the total substrate area on one side.

Now we estimate the P/S ratio for the whole tessellation based on a tight estimate of the P/S ratio for a single cell $P/S \le 4P/(P(D+2s) + \pi s^2)$. Using an equivalent form for an estimate of a single cell, we conclude that $P_i/S_i \le (4/(D+2s))(1 - ((\pi s^2)/((D+2s)P_i + \pi s^2))) \le (4/(D+2s))(1 - ((\pi s^2)/((D+2s)\max_i\{P_i\} + \pi s^2)))$ for any $i \in \{1, ..., N\}$. Applying Lemma 2, we conclude that $P/S \le (4/(D+2s))(1 - ((\pi s^2)/((D+2s)\cdot \max_i\{P_i\} + \pi s^2))$, or equivalently that $P/S \le (4\max_i\{P_i\})/((D+2s)\max_i\{P_i\} + \pi s^2)$. This estimate shows that $4/(D+2s)$ is not a tight bound, because $\max_i\{P_i\}$ is a finite number bounded from above by the perimeter of the silicon substrate.

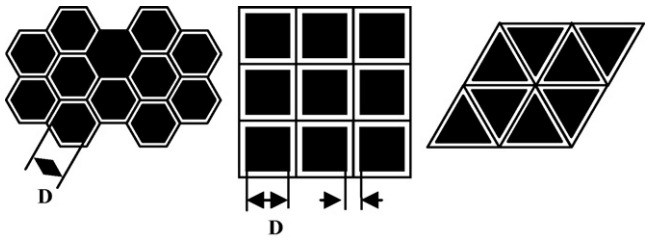

Fig. 9. Cell configurations based on the tessellations in Fig. 8.

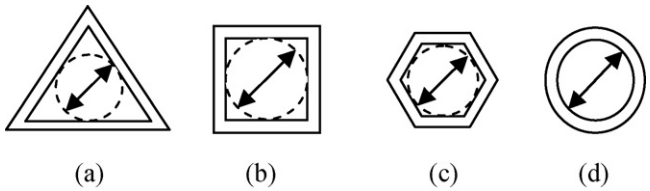

Fig. 10. (a) Triangle with inscribed circle of diameter D and walls of width $s/2$. (b) Square with inscribed circle of diameter D. (c) Hexagon with inscribed circle of diameter D. (d) Circle of diameter D.

In summary, we have two estimates for the P/S ratio for a hole configuration where each hole is a convex polygon with an inner diameter at least D, where the distance between two holes is at least s and where the distance from any hole to the substrate edge is at least $s/2$:

- $\frac{P}{S} \le \frac{4}{D+2s}$
- $\frac{P}{S} \le \frac{4}{D+2s}\left(1 - \frac{\pi s^2}{(D+2s)\cdot \max_i\{P_i\} + \pi s^2}\right)$.

In fact, these estimates are valid for any convex hole that satisfies the requirements on the wall width and the inner diameter, because any such hole can be approximated by a convex polygon.

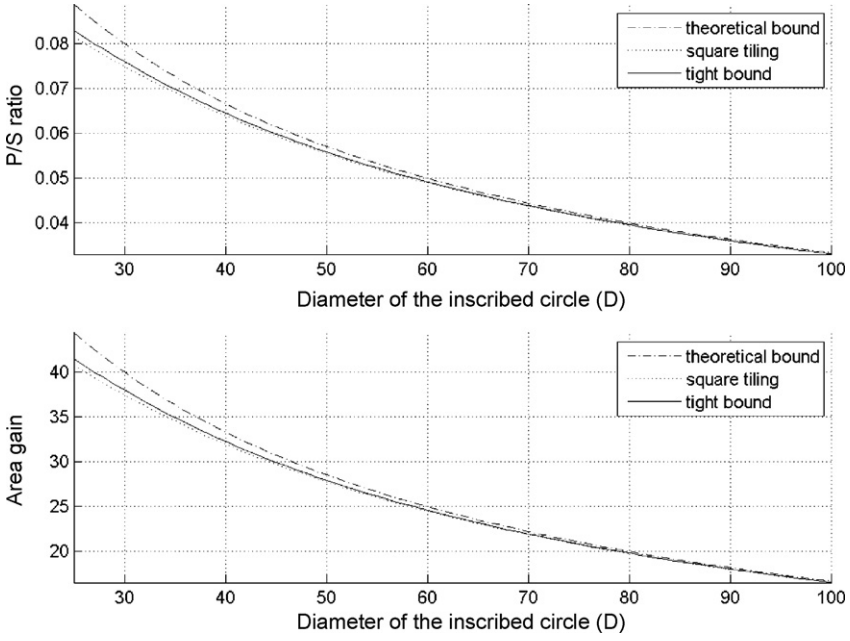

Fig. 11. P/S ratio and AG for square tiling: $s = 10$, $d = 500$ μm.

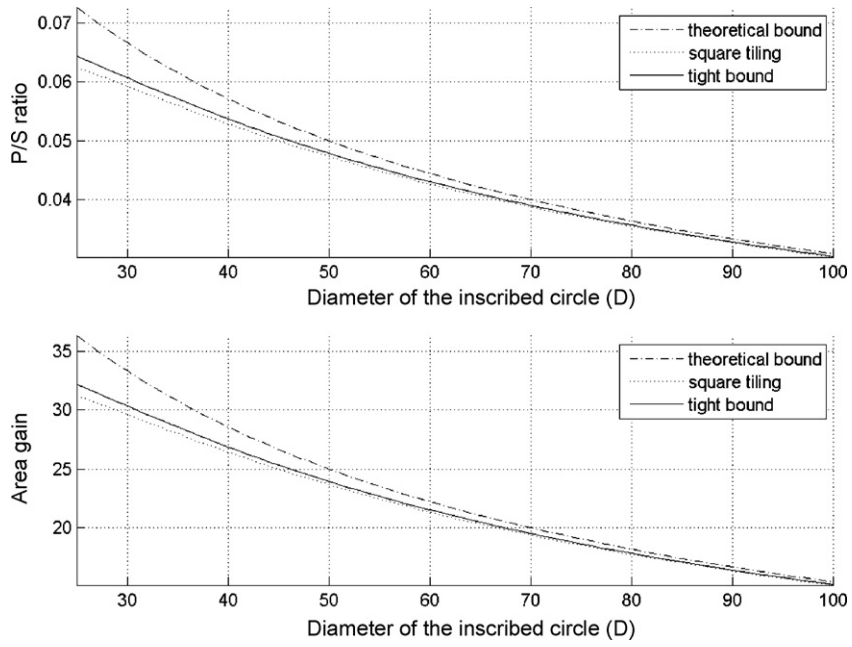

Fig. 12. *P*/*S* ratio and AG for square tiling: $s = 15$, $d = 500$ μm.

3. Analysis of different configurations

Next, we compare a number of hole configurations to the upper bound derived above. It is well known that there are three possible regular tessellations of the plane: triangles, squares and hexagons—see Figs. 8 and 9. The term "regular" denotes a tessellation by cells that satisfy the following requirements: each cell is a regular polygon, the "hole" is a regular polygon of the same form as the cell but smaller (since walls are not zero width), and all cells are equal. The term "smoothed" with reference to tessellation denotes cells that satisfy the following requirements: each hole is a regular polygon but the cell external boundary is not a regular polygon anymore. It consists of points located at the distance $s/2$ from the hole. In other words, we take the "hole" and perform a morphological operation of "opening" using a circle of diameter "s". The external boundary of the resulting cells has smooth corners, as seen in Figs. 14a, 15a and 16a. The union of the cells with smoothed corners does not cover the whole silicon surface. Union of these cells does cover the whole silicon surface.

We consider cell configurations which are based on these tessellations and shown in Fig. 10. These are: (a) triangle with inscribed circle of diameter D and walls with width $s/2$: $P_3 = 3\sqrt{3}D$, $S_3 = (3\sqrt{3}/4)(D+s)^2$, $P_3/S_3 = 4D/((D+s)^2)$; (b) a square with inscribed circle of diameter D: $P_4 = 4D$, $S_4 = (D+s)^2$, $P_4/S_4 = 4D/(D+s)^2$; (c) a hexagon with inscribed circle of diameter D: $P_6 = 2\sqrt{3}D$, $S_6 = (\sqrt{3}/2)(D+s)^2$, $(P_6/S_6) = (4D)/((D+s)^2)$; and (d) a circle of diameter D: $P_0 = \pi D$, $S_0 = (\pi/4)(D+s)^2$, $P_0/S_0 = 4D/((D+s)^2)$. Note that the same *P*/*S* ratio holds for the smallest convex figure that contains a

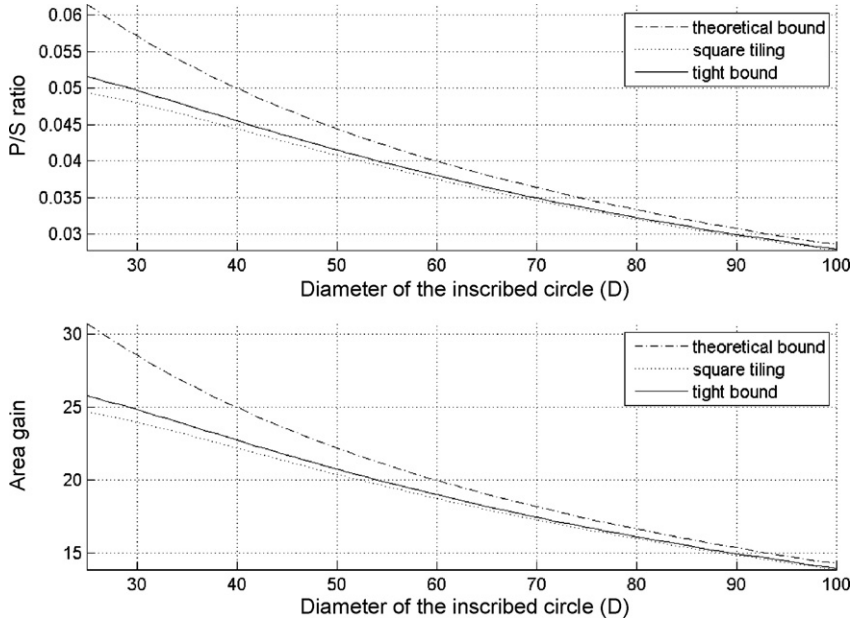

Fig. 13. *P*/*S* ratio and AG for square tiling: $s = 20$, $d = 500$ μm.

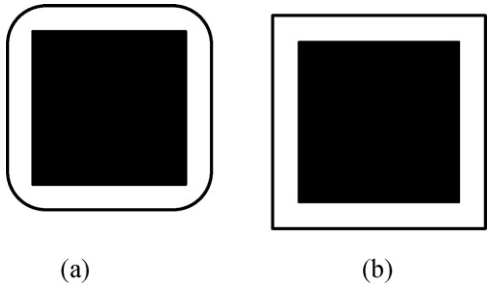

Fig. 14. (a) Square hole and the cell with the minimal area. (b) Cell with a P/S ratio larger than the P/S ratio of the cell used for regular tiling.

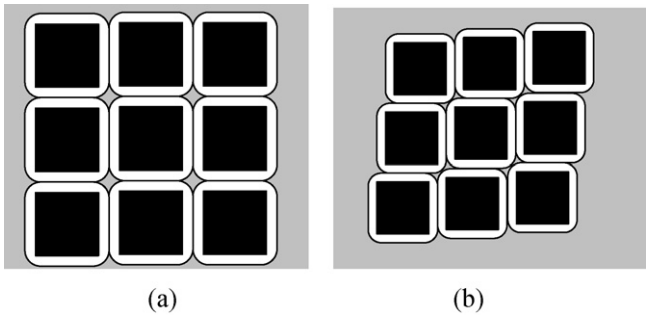

Fig. 15. Two different arrangements for tessellation of the plane using more of the optimal cells.

circle of radius D, i.e. the circle itself plus walls of $s/2$ width. Since tessellations considered by us consist of identical cells, the P/S ratio equals $(4D)/(D+s)^2$ for any of them. Let us see how far this P/S ratio is from the upper bound on the P/S ratio derived in Section 2.6. We plot graphs of P/S ratio as a function of $D \in [25, 100]$ for $s = 10$, 15, 20 in respectively Figs. 11–13. Based on the P/S ratio, we can compute the AG of a given hole configuration by multiplication of the P/S ratio by d. For illustration, the graphs plotted in these figures are for AG when d is 500 μm. The dotted line in the graph represents the P/S ratio $(4D)/(D+s)^2$, the dash-dot line is the upper bound $(4)/(D+2s)$ and the continuous line is the "tight bound" for all tessellations where the perimeter of each hole is less than or equal to $4D$. One can clearly see that all regular tessellations are equivalent.

Let us consider a square hole and a cell with the minimal area (their walls are exactly $s/2$ thick), Fig. 14a. The P/S ratio of this cell is larger than the P/S ratio of the cell used for regular tiling, Fig. 14b. Indeed, in the first case we have $P = 4D$ and $S = D^2 + 4D(s/2) + \pi(s/2)^2 = D^2 + 2Ds + (\pi/4)s^2$, whereas in the second case we have $P = 4D$ and $S = (D+s)^2$. The question is whether we can tessellate the plane using more of these optimal cells.

We consider the arrangement of these cells shown in Fig. 15a. The configuration of the holes is the same as in the regular tiling, but there is a space that is not covered by cells near the corners. The

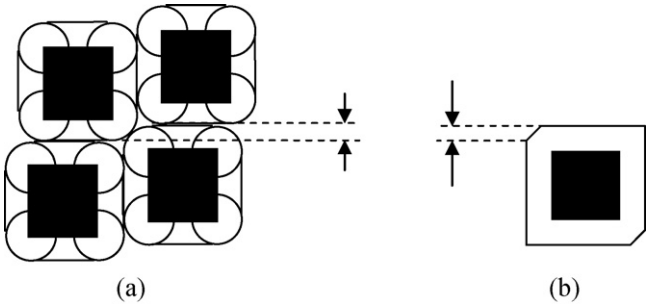

Fig. 16. (a) Fragment of the tiling in (b). (b) Cell for the tiling given in Fig. 17.

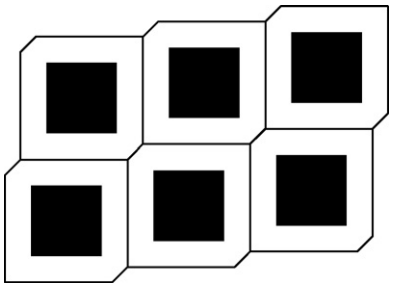

Fig. 17. Computation of the P/S ratio for this configuration.

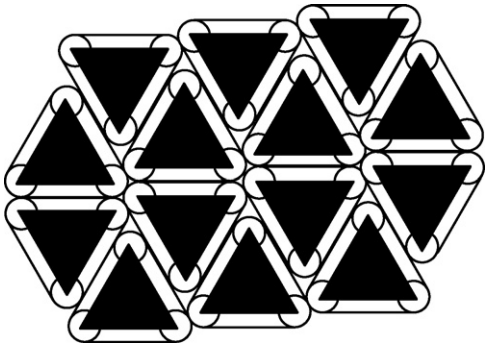

Fig. 18. Configuration of "smoothed triangular" cells for which the P/S ratio is better than that of a regular tessellation. The walls are exactly $s/2$ thick. Note that there areas that do not belong to any cell near cell corners.

P/S ratio for this hole arrangement can be computed as the ratio between the perimeter of a hole and the sum of the areas which is computed as the area of the cell plus the area of the non-filled area near the corner.

Now we consider another arrangement, shown in Fig. 15b. Here the non-filled area is smaller. Therefore, the P/S ratio is higher than in the regular tiling case, although it is smaller than the P/S ratio of a single cell. Following is a formal proof that this hole configuration is better than a regular tessellation.

Fig. 16a is a fragment of this tiling. The diameter of the small circles is s. First, we find the vertical displacement of the cells. It is not hard to compute it as that the vertical displacement is $s(\sqrt{2}-1)/(\sqrt{2})$. Then, we get the same hole configuration by tiling the plane with cells of the form shown in Fig. 16b. The tiling is shown in Fig. 17. For this tiling, it is easy to show that $P = 4D$ and $S = (D+s)^2 - s^2((\sqrt{2}-1)/\sqrt{2})^2$ and that the P/S ratio is $P/S = (4D)/((D+s)^2 - s^2((\sqrt{2}-1)/\sqrt{2})^2) = (4D)/((D+s)^2 - s^2((\sqrt{2}-1)^2/2)) = (4D)/(D^2 + 2Ds + s^2(\sqrt{2}-0.5))$.

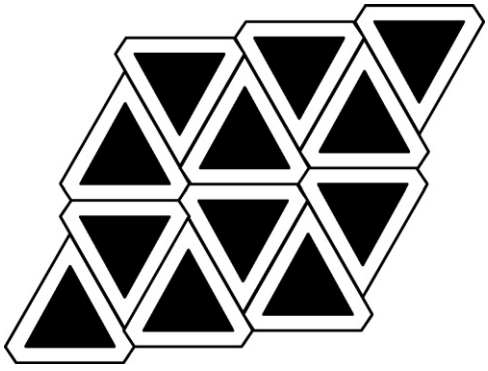

Fig. 19. Tiling of the plane by cells with the same configuration of holes as in Fig. 20. Unlike in Fig. 18, there are no non-filled areas near cell corners. The walls are at least $2/s$ thick.

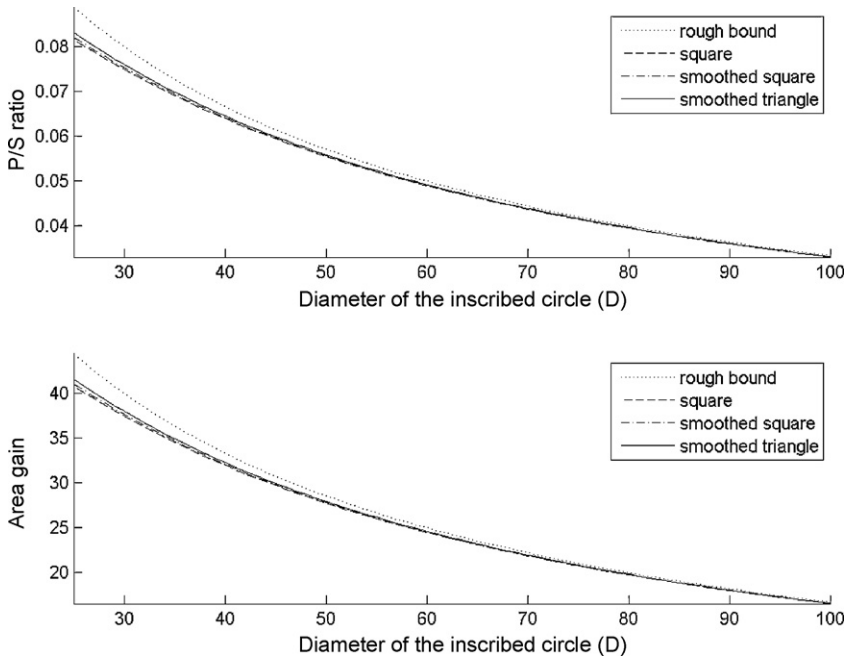

Fig. 20. P/S ratio and AG for smoothed square and triangle cells: $s = 10$, $d = 500$ μm.

Since $\sqrt{2} - 0.5 < 1$ we have $D^2 + 2Ds + s^2(\sqrt{2} - 0.5) < (D + s)^2$, therefore $P/S = (4D)/(D^2 + 2Ds + s^2(\sqrt{2} - 0.5)) > (4D)/(D + s)^2$.

The configuration of smoothed square holes provides a higher P/S ratio than any "regular tessellation" which satisfies the same requirements, i.e. has holes with internal diameter "D" and inter-hole distances not less than "s". Figs. 20–22 show plots of the P/S ratio of "square" and "smoothed square" tessellations.

3.1. Smoothed triangle tessellation

We can use the above approach to find a tessellation based on triangular holes in which the P/S ratio is better than that provided by a regular tessellation. It will also be better than that provided by the smoothed square tessellation.

We consider regular triangular holes and a cell with minimal area (with walls exactly $s/2$ thick). Then, we consider the cell arrangement shown in Fig. 18. This arrangement is not a tiling, since there are areas not covered by cells near the smoothed corners of the triangular cells. However, we can get the same hole configuration by tiling the plane with cells with the form shown in Fig. 19. For one cell, we have $P = 3\sqrt{3}D$ and $S = (3\sqrt{3}/4)(D + s)^2 - (s^2/(2\sqrt{3}))$. Therefore, $P/S = 4D/((D + s)^2 - (2/9)s^2)$. We compare this to the smoothed square tiling, where P/S was $(4D)/((D + s)^2 - s^2((\sqrt{2} - 1)/\sqrt{2})^2)$. We note that $(\sqrt{2} - 1/\sqrt{2})^2 \approx 0.0858$ where $2/9 \approx 0.2222$. That is, $P/S = (4D)/((D + s)^2 - (2/9)s^2) \geq (4D)/((D + s)^2 - s^2((\sqrt{2} - 1)/\sqrt{2})^2)$. We get a better P/S ratio than that received in

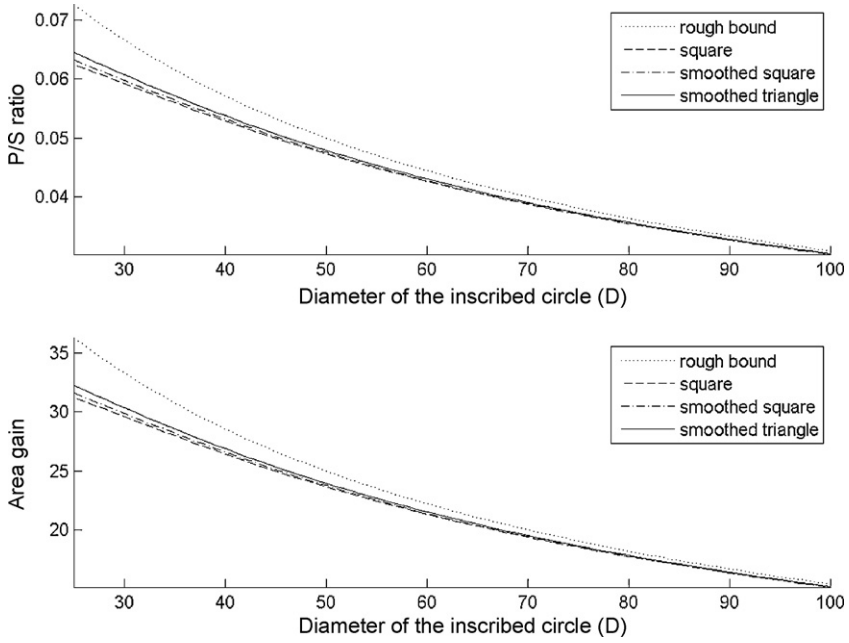

Fig. 21. P/S ratio and AG for smoothed square and triangle cells: $s = 15$, $d = 500$ μm.

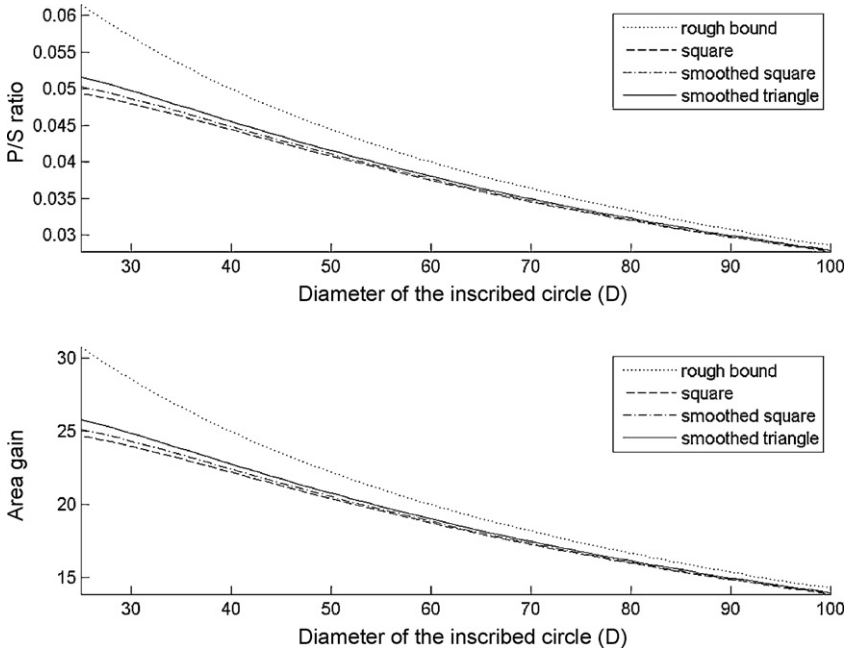

Fig. 22. P/S ratio and AG for smoothed square and triangle cells: $s = 20$, $d = 500$.

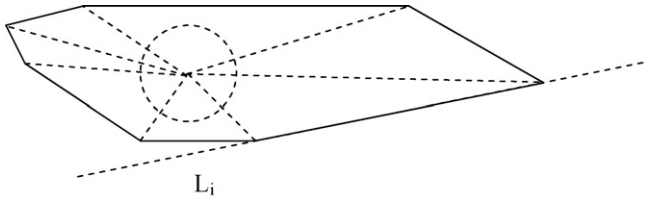

Fig. 23. Illustration for the proof of Lemma 4.

the smoothed square case. All of this is shown in the comparison charts in Figs. 20–22, which plot the P/S and the AG for three configurations: regular square tessellation, smoothed square tessellation and smoothed triangle tessellation.

In conclusion, the smoothed triangle tessellation produces the best AG for all compared configurations. It is important to remember that all these comparisons were made under the assumption that a minimal hole size is determined by the diameter of the inscribed circle. If in practice, smoothed square holes with internal diameter X can be fabricated and smoothed triangular holes can also be fabricated with internal diameter $Y > X$, then, it is possible that the smoothed square cells will produce a larger area gain.

Acknowledgment

A. Averbuch and M. Nathan gratefully acknowledge the support of the US-Israel Binational Science Foundation (BSF) through Grant # 2004403.

Appendix A.

Lemma 1. Let P_i, S_i $i \in \{1, 2\}$, be positive numbers such that $P_1/S_1 \le P_2/S_2$. Then, $P_1/S_1 \le (P_1 + P_2)/(S_1 + S_2) \le P_2/S_2$.

Lemma 2. Let N be a positive integer, $P_1, \ldots, P_N$ and $S_1, \ldots, S_N$ are positive numbers. We define $P = \sum_{i=1}^{N} P_i$ and $S = \sum_{i=1}^{N} S_i$. Then, there exists k, $l \in \{1, \ldots, N\}$ such that $P_k/S_k \le P/S \le P_l/S_l$.

Lemma 3. For any regular polygon with an inscribed circle of radius D, the ratio between the perimeter and the area is $4/D$.

Proof: Consider a N-side polygon. We connect each vertex to its center, thus dividing the polygon into N equilateral triangles. Each triangle has a "central" angle equal to $360/N$ degrees, and two angles near the base equal to $(180 - (360/N))(1/2) = 90 - (180/N)$. Denote $R = D/2$. Then, the area of each triangle equals $S_t = R^2 ctg(90 - (180/N))$. Then, the area of this polygon is $S = NR^2 ctg(90 - (180/N))$. The base of each

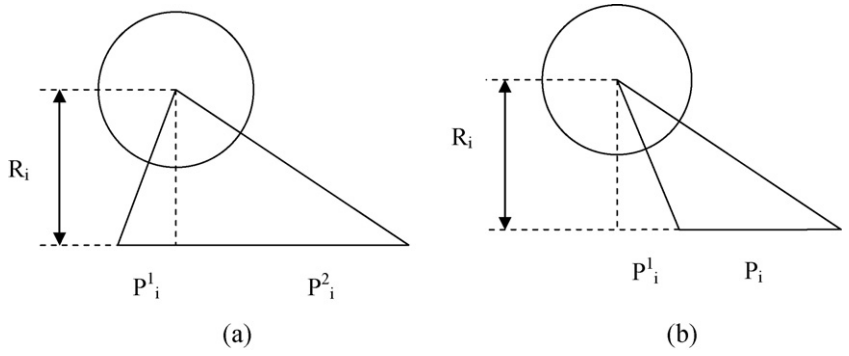

Fig. 24. Illustrations for the proof of Lemma 4.

triangle equals $2Rctg(90-(180/N))$, therefore, the perimeter $P=2NRctg(90-(180/N))$. Then, the ratio between the perimeter and the area of the polygon is $P/S=2/R=4/D$.

Lemma 4. For a convex polygon that contains a circle of diameter D, the ratio between the polygon perimeter P and the polygon area S satisfies $P/S \le 4/D$. This equality holds if and only if the polygon is bounded by lines tangent to the circle.

Proof: We connect the center of the polygon to its vertices thus dividing it into triangles, see Fig. 23. Assume that the polygon has N sides. We enumerate these sides and denote the length of the ith side by P_i. The area of the ith triangle is denoted by S_i The straight line L_i, which contains the ith side of a polygon, cannot intersect the inscribed circle. Indeed, the circle is located inside the polygon. It is known that a convex polygon lies completely in one of the half-planes to which L_i divides the plane. Now, if we consider a line that passes through the center of the circle and is orthogonal to L_i, two cases are possible: either the line crosses the ith side or not. We denote by R_i the distance from the center of the circle to L_i. Case 1 is shown in Fig. 24a and case 2 is shown in Fig. 24b.

In case 1, $S_i=(R_iP_i^1/2)+(R_iP_i^2/2)=(R_iP_i/2)$. In case 2, $S_i=(R_i(P_i+P_i^1)/2)-(R_iP_i^1/2)=(R_iP_i/2)$. Therefore, in any case we have $P_i/S_i=2/R_i$. Now, $R_i \ge D/2$ and, therefore, $1/R_i \le 2/D$. Then, for any $i\in\{1,\ldots,N\}$ we have $P_i/S_i \le 4/D$. The perimeter of the polygon is $P=\sum_{i=1}^{N}P_i$ and the area of the polygon is $S=\sum_{i=1}^{N}S_i$. By Lemma 2, there exists $j\in\{1,\ldots,N\}$ such that $P/S \le P_j/S_j$. Consequently, $P/S \le 4/D$. In the case when the polygon is bounded by lines tangent to the circle, we have $R_i=D/2$ for all $i\in\{1,\ldots,N\}$, therefore, $P_i/S_i=4/D$ for all $i\in\{1,\ldots,N\}$. By Lemma 2, there exists $k,l\in\{1,\ldots,N\}$ such that $P_k/S_k \le P/S \le P_l/S_l$. Consequently, $P/S=4/D$. Now, suppose that at least one line that bounds the polygon is not tangent to the circle. Then, there exists $k\in\{1,\ldots,N\}$ such that $P_k/S_k<4/D$. Then, $P_kD<4S_k$. Taking into account that $P_iD\le 4S_i$ for all $i\in\{1,\ldots,N\}$, we have $P_1D+\ldots+P_ND<4S_1+\ldots+4S_N$, that is $P/S<4/D$.

Lemma 5. Let N be a positive integer. Consider N convex polygons such that every polygon contains a circle of radius D. We enumerate them. We denote by P_i the perimeter of the ith polygon and by S_i the area of the ith polygon. We define $P=\sum_{i=1}^{N}P_i$ (total perimeter of all polygons) and $S=\sum_{i=1}^{N}S_i$ (total area of all polygons). Then, $P/S \le 4/D$.

Proof: By Lemma 2, there exists $j\in\{1,\ldots,N\}$ such that $P/S \le P_j/S_j$. Since all the polygons in the tiling are convex and contain a circle of radius D, we get from Lemma 4 that $P_i/S_i \le 4/D$ for any $i\in\{1,\ldots,N\}$. Therefore, $P/S \le 4/D$.

Lemma 6. Let P, S, S_H, D and s be positive numbers, such that $P/S_H \le 4/D$ and $S \ge S_H+P(s/2)$. Then, $P/S \le 4/(D+2s)$.

Proof: Since $S \ge S_H+P(s/2)$, we have $P/S \le P/(S_H+P(s/2))$. From the inequality $P/S_H \le 4/D$, we get $PD \le 4S_H \Rightarrow PD+2Ps \le 4S_H+2Ps \Rightarrow P(D+2s) \le 4(S_H+P(s/2)) \Rightarrow P/(S_H+P(s/2)) \le 4/(D+2s)$.

Lemma 7. Let N be a positive integer, P_1, ..., P_N and S_1, ..., S_N be positive numbers such that $P_i/S_i \le 4/D$ holds for any $i\in\{1,\ldots,N\}$. Let C_1, ..., C_N be numbers such that $C_i \ge S_i+P_i(s/2)$ for any $i\in\{1,\ldots,N\}$. We define $P=\sum_{i=1}^{N}P_i$ and $S=\sum_{i=1}^{N}C_i$. Then, $P/S \le 4/(D+2s)$.

Proof: From Lemma 6, $P_i/C_i \le 4/(D+2s)$ for any $i\in\{1,\ldots,N\}$. By applying Lemma 2 we get $P/S \le 4/(D+2s)$.

References

[1] M. Nathan, D. Haronian, E. Peled, "Micro-electrochemical cell", U.S. Patent 6,197,450 (2001).
[2] M. Nathan, D. Golodnitsky, V. Yufit, E. Strauss, T. Ripenbein, I. Shechtman, S. Menkin, E. Peled, MRS Proc. 835 (2004) K.10.10.1–K10.10.6.
[3] M. Nathan, D. Golodnitsky, V. Yufit, E. Strauss, T. Ripenbein, I. Shechtman, S. Menkin, E. Peled, J. Microelectromech. Syst. 14 (5) (2005) 879–885.
[4] D. Golodnitsky, V. Yufit, M. Nathan, I. Shechtman, T. Ripenbein, E. Strauss, S. Menkin, E. Peled, J. Power Sources 156 (2006) 281–287.
[5] D. Golodnitsky, M. Nathan, V. Yufit, E. Strauss, K. Freedman, L. Burstein, A. Gladkich, E. Peled, Solid State Ionics 177 (2006) 2811–2819.
[6] V. Yufit, D. Golodnitsky, L. Burstein, M. Nathan, E. Peled, Solid State Electrochem. 12 (3) (2008) 273–285.
[7] T. Ripenbein, D. Golodnitsky, M. Nathan, E. Peled, J. Appl. Electrochem. 40 (2010) 435–444.
[8] M. Nathan, Curr. Pharm. Biotechnol. 11 (4) (2010) 404–410.
[9] P.H.L. Notten, F. Roozeboom, R.A.H. Niessen, L. Baggetto, Adv. Mater. 19 (24) (2007) 4564–4567.
[10] L. Baggetto, R.A.H. Niessen, F. Roozeboom, P.H.L. Notten, Adv. Funct. Mater. 18 (7) (2008) 1057–1066.